Risk-Aware Limited Rerouting and Demand Allocation in Structured UAM Airspace

Rami Sabbagh*[1] and Jack Haddad[2]

[1]Technion Autonomous Systems Program (TASP)
[2]Technion–Israel Institute of Technology

Short summary

Urban Air Mobility (UAM) operations in structured airspace face a key challenge in managing congestion. This paper proposes a departure control framework with limited rerouting that identifies high-risk paths using a conflict-based risk metric and shifts part of their demand to lower-risk existing paths through short detours. The approach is evaluated in the LAAT-Flow simulation environment under three demand allocation strategies, namely full, fixed, and dynamic allocation. The results show that all strategies reduce overall network risk. Dynamic allocation provides the most stable improvement as more paths are rerouted, while full allocation initially achieves strong risk reduction but may create new bottlenecks when demand is concentrated on alternative paths. These safety improvements come at the cost of increased energy consumption due to longer alternative paths. The findings demonstrate that limited rerouting with adaptive allocation offers a practical approach for improving safety in corridor-based UAM operations.
Keywords: Conflict-based risk, Conflict management, Demand allocation, Limited rerouting, Structured airspace, Urban air mobility

1 Introduction

Urban Air Mobility (UAM) is gaining increasing attention as a new mode of transportation capable of transforming passenger and cargo movement within urban environments. Recent advances in electrification, automation, and electric vertical take-off and landing (eVTOL) aircraft design have enabled UAM to provide safe, sustainable, and scalable aerial solutions for urban transit, logistics, and emergency services Cohen et al. (2021); Long et al. (2023). With the rise of UAM operations comes a critical need to design and manage urban airspace. For safe operations in low-altitude airspace, concepts of operation (ConOps) for unmanned aircraft system traffic management (UTM) are being introduced, such as NASA (2021). These concepts have been examined, reviewed, and evaluated across various factors, showing that the structure of the airspace directly influences its safety, efficiency, and capacity Bauranov and Rakas (2021).

One such ConOps is tube-based operations, which require planning and design techniques for the airspace 'tubes'. This concept was introduced in EUROCONTROL (2018), where structured paths are described as pre-planned pathways. One approach generates tube paths using a priority-driven sequential planner that optimizes a weighted objective function (e.g., noise, risk, airspace utilization) He et al. (2022). This was later extended to a distributed framework that coordinates paths via congestion pricing to balance individual path quality with system-level performance He et al. (2024). With these approaches comes the need for simulation frameworks capable of evaluating how UAM operates and of supporting the design and optimization of UAM systems Safadi and Haddad (2024).

To this end, a collaborative study with a research group from the City University of Hong Kong was conducted to evaluate the performance of three urban airspace configurations for UTM: (i) Structured Corridor without Intersections, (ii) Structured Corridor with Intersections, and (iii) Unstructured Free-Flight, in a test area of Mong Kok, a dense urban district in Hong Kong Bai et al. (2026). The structured designs were generated by the algorithm He et al. (2022, 2024), and the evaluation was conducted using the Low Altitude Air Transport Flow (LAAT-Flow) framework Safadi and Haddad (2024). The results showed that as demand increases, most predicted conflicts (called as "predicted collisions" in Bai et al. (2026)) occur at the origin-destination (OD) nodes, while en-route conflicts depend on the airspace structure design. In addition, no single airspace design outperformed the other designs in all evaluation metrics, such as predicted collisions, energy, and

time. These findings highlight the need for operational strategies that can manage congestion and balance these trade-offs without requiring a redesign of the airspace structure.
To address this need, this paper proposes a departure-control framework with limited rerouting for UAM that focuses on rerouting and demand allocation, with a rerouting strategy that temporarily redirects flights through intermediate vertiports when direct corridors are congested. Previous works have addressed rerouting and departure control, but few integrate both in UAM.
The main contribution of this paper is threefold. First, we propose a limited rerouting mechanism for structured UAM airspace that mitigates congestion-related conflict risk without requiring a redesign of the underlying corridor network. Second, we introduce a path-level risk-based selection process to identify both rerouting targets and feasible low-risk alternatives. Third, we compare three allocation strategies – full, fixed, and dynamic – and show how adaptive allocation can provide more robust risk reduction when several high-risk paths are rerouted.

Related Work

In UAM operations, conflict management plays an important role in traffic management for safe flight operations. One of the key approaches is Demand Capacity Balancing (DCB), which prevents vertiport congestion by automatically adjusting flight schedules before departure Lee et al. (2022). Beyond departure delays, airborne delay is introduced by temporarily reducing the cruise speed, thereby shifting part of the delay into the air rather than keeping the vehicle on the ground Moolchandani and Lee (2024).
Another approach is a dynamic DCB in the U-space that simultaneously reroutes flights, reconfigures airspace, and assigns delays when congestion is detected Tang et al. (2022). A Collaborative Air Traffic Flow Management framework simultaneously assigns delays or reroutes flights while dynamically adjusting airspace sector configurations, with the objective of minimizing total delay and operational costs Xu et al. (2020).
A probabilistic model is used to improve conflict detection under uncertainty, combined with network analysis to identify critical flight plans, followed by optimization over departure time and speed Meng et al. (2025).
With advances in artificial intelligence, several AI-driven approaches have emerged. A UTM system framework based on hybrid AI performs DCB and improves automated decision-making for drone traffic in dense urban low-altitude airspace Y. Xie et al. (2021). A follow-up work introduced Tabu Search combined with A* path planning for 2D dynamic rerouting as part of the DCB process Y. Xie et al. (2023a). This was extended to integrated 4D trajectory planning, enabling dynamic and adaptive DCB strategy optimization using hybrid AI algorithms Y. Xie et al. (2023b).
At the arrival stage, the concept of vertiport holding points is introduced, together with three scheduling strategies for efficient aircraft arrival management Song and Yeo (2021).

2 Methodology

In structured airspace design, congestion management in corridor-based UAM systems is one of the main challenges. This research proposes a design that improves traditional departure controllers by integrating a limited rerouting mechanism. When designing structured airspace, corridor paths can become highly congested due to design constraints, environmental or terrain limitations, or the lack of demand-aware planning. Generating entirely new corridor paths may be infeasible because of these constraints or due to the computational complexity of path generation algorithms.
Instead, the proposed limited rerouting mechanism identifies congested (and therefore potentially risky) paths and redirects part of the demand to less congested existing paths within the network. This approach avoids full path redesign and requires only the creation of short detour segments connecting the original path to an alternative corridor.
In this paper, we focus on the rerouting and demand allocation components of the framework. Two allocation strategies are implemented, namely fixed and dynamic allocation, while full allocation is used as a reference case.
The overall structure of the proposed approach is as follows: identification of congested paths, followed by rerouting, and finally demand allocation.

Congestion Identification

There are multiple ways to identify congestion in corridor-based airspace. In this work, we use predicted conflict detections as an operational risk indicator, since paths with a high number of such detections correspond to regions of increased traffic interaction, which are often associated with high congestion levels H. Xie et al. (2025). Thus, the proposed metric should be interpreted as a surrogate indicator of congestion-related conflict exposure rather than as a direct physical measure of congestion such as density, delay, or queue length.
In this work, we use predicted conflict events as an operational risk indicator, since UAVs estimate future positions based on filtered state estimates and trigger a repulsive avoidance mechanism when a potential collision is predicted. Paths with a high number of such predicted events correspond to regions of increased traffic interaction, which are often associated with higher congestion levels H. Xie et al. (2025). Thus, the proposed metric should be interpreted as a surrogate indicator of congestion-related conflict exposure rather than as a direct physical measure of congestion such as density, delay, or queue length
The collision count is defined as the number of predicted detection-trigger events along a path. Collision detection is implemented using a filtered position-based scheme, inspired by the decentralized control framework in Quan et al. (2021) and adopted in the simulation framework in Safadi and Haddad (2024). In this approach, both the detection and safety radii are centered around the UAV's filtered position, which serves as a proxy for its predicted future location. When two aircraft enter each other's detection zone based on these filtered positions, a repulsive control action is applied to separate them. As a result, the detected events represent predicted conflicts rather than actual physical collisions. The number of such events is then used as a measure of interaction intensity along each path.
We define a conflict-based risk metric, commonly expressed as a rate Bijjahalli et al. (2022); Yang et al. (2024), that captures both the number of predicted conflicts and the number of aircraft assigned to a given path. Let C_i denote the total number of predicted conflict detections associated with path i and let N_i represent the aggregated number of aircraft assigned to that path. Then, the risk is defined as:

$$R_i = \frac{C_i}{N_i} \tag{1}$$

Since the network is evaluated under varying demand allocations, both C_i and N_i represent aggregated predicted conflicts and aggregated aircraft counts, respectively, and the following holds:

$$N_i = \sum_{k=1}^{K} n_i^{(k)} \tag{2}$$

where $n_i^{(k)}$ is the number of aircraft assigned to path i in run k.
The overall network risk is defined as:

$$\bar{R} = \frac{\sum_{i=1}^{N} C_i}{\sum_{i=1}^{N} N_i} \tag{3}$$

We also define the weighted contribution of each path to the network risk as:

$$R_i^w = \frac{N_i R_i}{\sum_{j=1}^{N} N_j} = \frac{C_i}{\sum_{j=1}^{N} N_j}, \qquad \sum_{i=1}^{N} R_i^w = \bar{R} \tag{4}$$

The metric R_i captures the average number of predicted conflict detections per aircraft assigned to path i, whereas R_i^w measures the contribution of path i to the aggregate network risk. The latter is used to prioritize rerouting candidates, since a path may have a high individual risk but a limited network-level effect if its demand is low.

Rerouting

With the risk metrics, the limited rerouting mechanism constructs detour paths that connect high-risk paths to lower-risk alternatives within the network. In this way, a portion of the demand is shifted to these low-risk paths to relieve the original path. The general concept of the rerouting strategy is illustrated in Fig. 1.
The first step in the limited rerouting mechanism is to identify the set $\mathcal{R}$ of highest-risk paths. For each risky path $r \in \mathcal{R}$, the algorithm constructs a candidate set $\mathcal{C}_r$ of rerouting alternatives. To

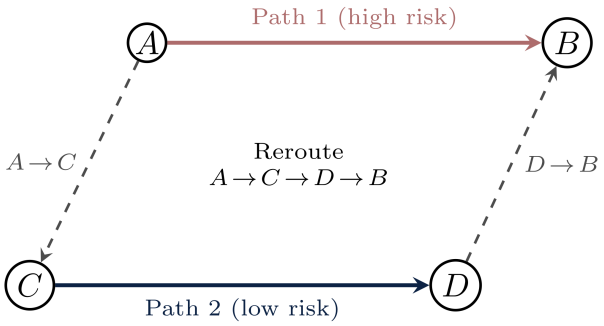


Figure 1: Illustration of the limited rerouting mechanism. Demand assigned to a high-risk path ($A \to B$) is partially redirected to a lower-risk path ($C \to D$) through intermediate connections ($A \to C$ and $D \to B$), forming an alternative path ($A \to C \to D \to B$).

avoid rerouting demand to paths that already contribute substantially to the overall network risk, the candidate set is filtered using a weighted-risk threshold, consistent with the safety requirements of UTM operations NASA (2021); Du et al. (2024). Only candidate paths satisfying $R_m^w \leq R_{\text{th}}$ are retained. The threshold is heuristically defined as:

$$R_{\text{th}} = \frac{\bar{R}}{N} \tag{5}$$

which corresponds to the average per-path contribution to the aggregate network risk.
For each candidate path m, a heuristic score is computed based on the Euclidean distance between the origin and destination of the risky path and those of the candidate path, together with a path-length compatibility term. Let O_r and D_r denote the origin and destination of risky path r, and let O_m and D_m denote those of candidate path m. The origin and destination distances are defined as:

$$d_O^{(r,m)} = \|O_r - O_m\| \,, \qquad d_D^{(r,m)} = \|D_r - D_m\| \tag{6}$$

The reroute candidate is the path with the minimum score:

$$m_r^\star = \arg\min_{m \in \mathcal{C}_r} S_{r,m} \tag{7}$$

where

$$S_{r,m} = w_1 \left(\widehat{d_O^{(r,m)}} + \widehat{d_D^{(r,m)}} \right) \; + \; w_2 \left(1 - \widehat{\frac{L_m}{L_r}} \right). \tag{8}$$

Here, $\widehat{(\cdot)}$ denotes min-max normalization over the candidate set $\mathcal{C}_r$, and the weights w_1 and w_2 reflect the relative importance of geometric compatibility and path-length similarity, respectively. After the best candidate is chosen, a path planning search is performed using the A* algorithm Hart et al. (1968). Since the network is designed such that departure and landing at each vertiport are performed vertically, the start and end points are defined at the vertiport operation altitude. The search exploration uses a Euclidean-based weighted heuristic function that penalizes vertical motion to keep the exploration mainly in the horizontal plane. This significantly simplifies the 3D search problem. Accordingly, the start and end nodes can be defined as follows, where H_r denotes the departure/landing altitude of path r:

1. From the origin of the risky path to the candidate path:

$$\text{Start: } O_r = (x_r^o, y_r^o, h_r^o), \quad \text{Goal: } O_{m_r^\star} = (x_{m_r^\star}^o + \Delta x,\; y_{m_r^\star}^o + \Delta y,\; H_r)$$

2. From the candidate path back to the destination of the original path:

$$\text{Start: } D_{m_r^\star} = (x_{m_r^\star}^d + \Delta x,\; y_{m_r^\star}^d + \Delta y,\; H_r), \quad \text{Goal: } D_r = (x_r^d, y_r^d, h_r^d)$$

The offset $(\Delta x, \Delta y)$ is chosen such that:

$$\Delta x^2 + \Delta y^2 = {r_{\text{offset}}}^2$$

where r_{offset} is a tunable safety radius parameter that ensures a bias offset away from the candidate's origin and destination points, so the merge occurs at a safe distance from the departure and landing altitude. The final step is to connect the generated detour segments with the selected candidate corridor and construct the complete rerouted alternative.

Demand Allocation

The purpose of rerouting is to relieve the original high-risk path by shifting part of its demand to the rerouted alternative. In this work, two allocation strategies are considered: (i) fixed allocation and (ii) dynamic allocation. In addition, full allocation, in which all demand is assigned to the rerouted alternative, is used as a reference case.
In both cases, a logit-based approach is used to allocate the demand. Since the original path and the rerouted alternative share common segments, the basic multinomial logit (MNL) model cannot be used, as it assumes independence between alternatives. Therefore, we consider overlap-aware models Cascetta et al. (1996); Ben-Akiva et al. (2004):

1. C-logit:
$$P_a = \frac{\exp\left(-\theta(J_a + CF_a)\right)}{\sum_{b\in\{o,\rho\}} \exp\left(-\theta(J_b + CF_b)\right)}$$

2. Path-Size Logit (PSL):
$$V_a = -\theta J_a + \beta \ln(PS_a)\,, \quad P_a = \frac{\exp(V_a)}{\sum_{b\in\{o,\rho\}} \exp(V_b)}$$

where P_a is the choice probability of alternative a, $a \in \{o, \rho\}$ denotes the original (o) or rerouted (ρ) alternative, θ is the sensitivity parameter, J_a is the cost associated with path a, CF_a is the C-logit commonality factor, V_a is the systematic utility, PS_a is the path-size factor, and β is the PSL coefficient.
Since the allocation problem involves only two alternatives, the C-logit model correction is assumed to affect both alternatives similarly and is therefore neglected in the present implementation. In addition, because the shared segments are relatively short in the considered network ($L_{ab} \ll L_a, L_b$), the PSL correction is expected to be small. Under these assumptions, both overlap-aware formulations reduce approximately to the basic MNL model:

$$P_a = \frac{\exp(-\theta J_a)}{\sum_{b\in\{o,\rho\}} \exp(-\theta J_b)} \tag{9}$$

Based on this formulation, the two allocation strategies are defined as:

1. **Fixed Allocation**

   In this case, the demand is distributed according to the choice probability Prashker and Bekhor (2004):
   $$D_a = P_a \cdot D_{\text{total}} \tag{10}$$
   where P_a follows Eq. 9, and the cost is defined as:
   $$J_a = w_R \widehat{R}_a^w + w_L \widehat{L}_a\,, \tag{11}$$
   where $\widehat{R}_a^w$ is the normalized weighted risk, $\widehat{L}_a$ is the normalized path length, and w_R and w_L are the corresponding weighting coefficients, with $w_R + w_L = 1$.
   For the original path, $R_o^w = R_r^w$ is obtained from the network, as computed in the previous step where the risk is evaluated. For the rerouted alternative, its weighted risk contribution is not directly available from the baseline network. We therefore estimate it heuristically using the weighted risk of the selected candidate path $m_r^\star$, scaled by the fraction of the rerouted path that overlaps with that candidate corridor: $R_\rho^w = R_{m_r^\star}^w \cdot \frac{L_{\rho m_r^\star}}{L_{m_r^\star}}$. This approximation assumes that conflict exposure is proportional to the length traveled on the shared corridor segment. As for L_a, the LAAT simulation uses the energy model in Thibbotuwawa et al. (2019). For simplicity, and under the assumption of constant cruise speed, the energy consumption can be approximated as proportional to the path length, i.e., $\mathcal{E}_a \propto L_a$.

2. **Dynamic Allocation**

Dynamic allocation extends the fixed-allocation formulation by making the routing decision sequentially at each departure event rather than assigning the demand split in advance. At each departure event n, occurring at time t_n, the aircraft associated with the considered risky path r is assigned to one of the two alternatives. This decision is represented by the binary variable $u_n \in \{0, 1\}$, where $u_n = 1$ denotes assignment to the rerouted alternative and $u_n = 0$ denotes assignment to the original path.

The decision is based on time-dependent logit probabilities:

$$P_a(t_n) = \frac{\exp(-\theta J_a(t_n))}{\sum_{b\in\{o,\rho\}} \exp(-\theta J_b(t_n))}\,, \qquad a \in \{o, \rho\}\,, \tag{12}$$

where $J_a(t_n)$ denotes the time-dependent cost of alternative a at departure event n.

The assignment is implemented deterministically by selecting the alternative with the higher probability:

$$u_n = \begin{cases} 1, & \text{if } P_\rho(t_n) > P_o(t_n)\,, \\ 0, & \text{otherwise}\,. \end{cases} \tag{13}$$

Thus, the logit formulation is used as a smooth decision rule rather than a stochastic route-choice model. The time dependent $J_a(t_n)$ follows the weighted structure of Eq. (11), but is evaluated dynamically based on the current traffic state and predicted evolution over a finite horizon H:

$$J_a(t_n) = w_R \widehat{R}_a^{\,w}(t_n, H) + w_E \widehat{\mathcal{E}}_a(t_n, H)\,, \tag{14}$$

where $\widehat{R}_a^{\,w}(t_n, H)$ denotes the normalized weighted risk and $\widehat{\mathcal{E}}_a(t_n, H)$ denotes the normalized dynamic energy cost, while w_R and w_E are the corresponding weighting coefficients.

Each cost component is decomposed into a history term, representing the accumulated cost up to the current departure time t_n, and a prediction term that estimates the future evolution over the horizon H. The dynamic formulation exploits the current traffic state and predicts the system evolution over the horizon H, allowing both risk and energy to be evaluated explicitly at each departure event.

Accordingly, the normalized dynamic energy cost is defined as:

$$\widehat{\mathcal{E}}_a(t_n, H) = \mathrm{Norm}\big(\mathcal{E}_a^{\mathrm{hist}}(t_n^-) + \mathcal{E}_a^{\mathrm{pred}}(t_n, H)\big) \tag{15}$$

where $\mathcal{E}_a^{\mathrm{hist}}(t_n^-)$ is the accumulated energy prior to t_n, and $\mathcal{E}_a^{\mathrm{pred}}(t_n, H)$ is the predicted energy over the horizon.

Similarly, the normalized dynamic risk is obtained as

$$\widehat{R}_a^{\,w}(t_n, H) = \mathrm{Norm}\big(R_a^{\,w}\big(t_n, H; C_a^{\mathrm{pred}}(t_n, H), C_a^{\mathrm{hist}}(t_n), N_a^{\mathrm{hist}}(t_n), N_a^{\mathrm{pred}}(t_n, H)\big)\big) \tag{16}$$

where $C_a^{\mathrm{hist}}(t_n)$ and $C_a^{\mathrm{pred}}(t_n, H)$ denote the historical and predicted conflict contributions, while $N_a^{\mathrm{hist}}(t_n)$ and $N_a^{\mathrm{pred}}(t_n, H)$ represent the corresponding numbers of aircraft. The weighted conflict risk $R_a^w(\cdot)$ is evaluated according to the formulation in Eq. (4).

The history term penalizes repeated use of an already overused alternative, while the prediction term evaluates the expected future rerouting cost over horizon H.

3 Results and discussion

Simulation Setup

The evaluation was conducted over $K = 60$ runs, where in each run the aircraft demand was randomly allocated among the $N = 15$ paths. The simulation time step was fixed at 0.5 seconds, and the network demand profile was set as a constant inflow of $Q_{\mathrm{in}} = 0.1$ [aircraft/sec] over a total duration of 30 minutes. Aircraft in the simulation were modeled as UAVs, with a maximum speed of 20 [m/s], and were controlled using fixed trajectory tracking gains.

Unless stated otherwise, all model parameters were kept fixed throughout the experiments. The cost weights were set to $w_R = w_L = 0.5$ for the fixed allocation model and $w_R = w_E = 0.5$ for the dynamic allocation model. The rerouting candidate score weights were set to $w_1 = w_2 = 0.5$. The logit sensitivity parameter was set to $\theta = 1$, the prediction horizon was $H = 180\,\mathrm{s}$, and the rerouting offset radius was set to $r_{\mathrm{offset}} = 100\,\mathrm{m}$.
The evaluation metrics considered in this study are energy consumption and risk. Three different allocation strategies are evaluated: (i) full allocation to the rerouted alternative, (ii) fixed allocation, and (iii) dynamic allocation.
All strategies are compared against a baseline scenario with no rerouting. The comparison is applied to the top four high-risk paths, with rerouting introduced progressively from the highest-risk path to the top four paths. This progressive implementation allows isolating the marginal effect of limited rerouting as its spatial scope expands. The analysis is performed for a single network configuration and demand level, so the reported trends should be interpreted as scenario-dependent.

Results

This section presents the results of the rerouting and allocation strategies. The first step is to identify congested paths using the defined risk metrics. Fig. 2 illustrates the results over the K runs for the baseline scenario, where no rerouting is applied. It presents, for each path, the aggregated conflict count, aggregated aircraft count, and the weighted risk computed according to Eq. 4, along with the total network risk.
The results show that path 13 has the highest contribution to the overall network risk, while path 6 has the lowest. Accordingly, the top four high-risk paths selected for rerouting are paths 13, 12, 14, and 7. The overall network risk is $\bar{R} = 0.83\,[\frac{\text{pred. coll.}}{\text{aircraft}}]$.
These results show that the network risk is concentrated in a small subset of paths, highlighting potential value of limited rerouting.
After identifying the top four high-risk paths, the limited rerouting mechanism selected the best rerouting alternative for each of them. The best candidates for paths 13, 12, 14, and 7 are paths 11, 6, 5, and 2, respectively. The weighted risk values of these candidate paths can be seen in Fig. 2, where all selected alternatives remain below the threshold R_{th}.
As an example, the rerouting output generated for path 12 is illustrated in Fig. 3.
With the alternative path generated, total energy and network risk are evaluated to quantify the impact of the demand allocation strategies and the limited rerouting mechanism.
The overall network risk is shown in Fig. 4.
The results show that when only one path is rerouted, full allocation achieves the largest reduction in network risk. As the number of rerouted paths increases, the network risk continues to decrease for all three allocation strategies. However, when four paths are rerouted, the performance of full allocation deteriorates relative to the three-path case. A plausible explanation is that full allocation shifts all demand to the rerouted alternative, which initially removes risk from the original path but may subsequently create new hotspots along the alternative corridor due to demand concentration. Although dynamic allocation is initially outperformed by full allocation, its performance remains more stable as the rerouting scope expands. In the four-path rerouting case, it achieves the largest risk reduction among the tested strategies. This likely reflects its adaptive nature, since the allocation is updated at each departure event based on current path conditions, which helps redistribute demand and avoid creating new hotspots.
The fixed-allocation strategy generally performs worst among the three tested strategies. Because it uses the same allocation ratio throughout the simulation, it cannot adapt to evolving network conditions and therefore provides a smaller reduction in risk. Overall, all three allocation strategies reduce the network risk relative to the baseline, indicating that the proposed limited-rerouting mechanism is effective in shifting demand away from high-risk paths.
The total network energy is shown in Fig. 5. All allocation strategies increase the total network energy, and the increase becomes larger as more paths are rerouted. This is expected because limited rerouting generates alternative trajectories that are generally longer than the original paths, and longer traveled distances lead to higher energy consumption. Among the tested strategies, full allocation produces the largest energy increase, since it shifts all demand to the alternative paths without explicitly accounting for path efficiency. In contrast, the dynamic and fixed strategies lead to smaller increases because only part of the demand is rerouted. These results highlight a trade-off between operational safety, represented here by conflict-based risk reduction, and efficiency, represented by total energy consumption.

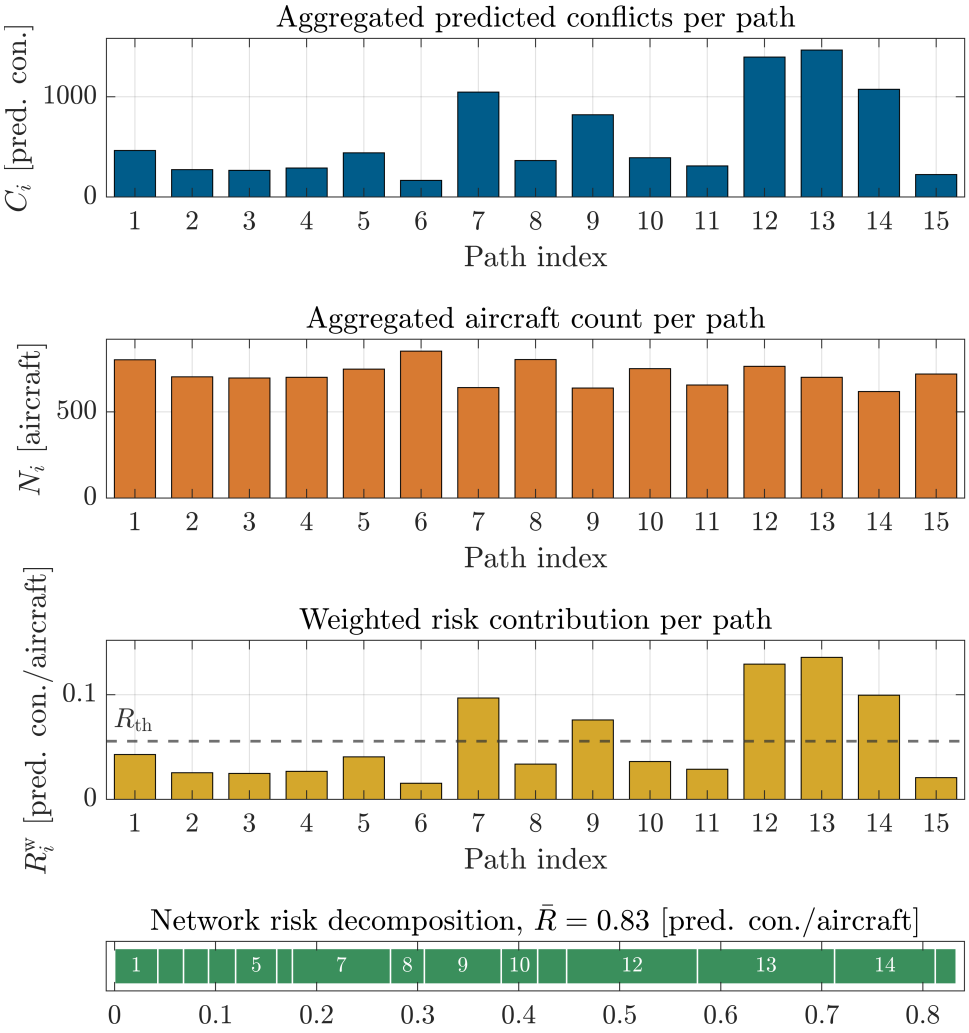


Figure 2: Baseline results without rerouting. The figure shows, for each path, the aggregated conflict count, aggregated aircraft count, and weighted risk, as well as the overall network risk.

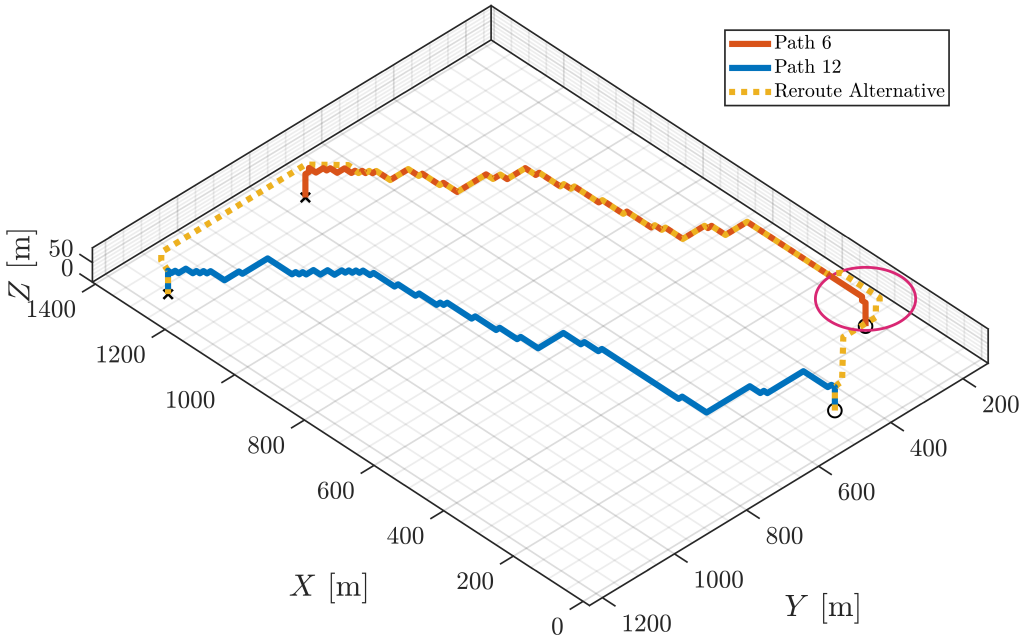


Figure 3: Example of the rerouting outcome for path 12. The original path (blue) is partially rerouted through a lower-risk candidate path (orange), forming a detour (dashed). The highlighted region indicates the merging point, where the detour connects to the candidate path using r_{offset}.

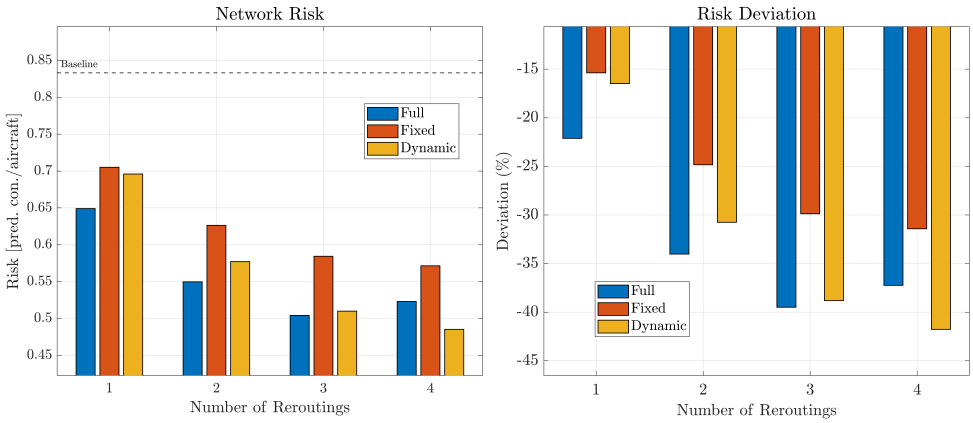


Figure 4: Network risk (left) and relative risk deviation (right) as a function of the number of rerouted paths for the three allocation strategies.

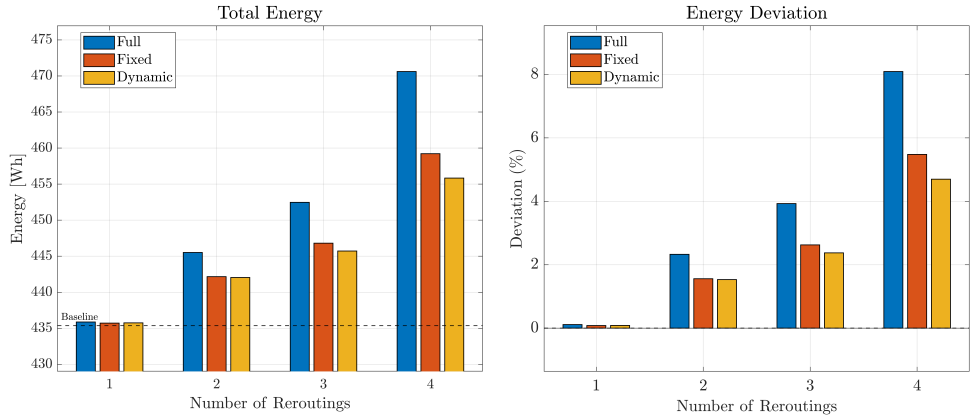


Figure 5: Total network energy (left) and relative energy deviation from the baseline (right) for the three allocation strategies as the number of rerouted paths increases.

4 Conclusions

This paper presented a limited-rerouting framework for structured Urban Air Mobility networks. The approach addresses congestion-related conflict management by identifying high-risk paths using a conflict-based risk indicator and redirecting part of their demand to lower-risk existing corridors, thereby avoiding a full redesign of the airspace structure. The simulation results showed that limited rerouting reduces network risk under all tested allocation strategies. Among these strategies, dynamic allocation provided the most robust performance as the rerouting scope increased, whereas full allocation achieved strong initial improvement but became less effective when additional paths were rerouted, likely because it concentrates demand on alternative corridors. Fixed allocation produced smaller improvements because it cannot adapt to evolving network conditions. These benefits came at the cost of higher total network energy consumption, since rerouted trajectories are generally longer than the original ones. Overall, the findings suggest that limited rerouting, especially when combined with adaptive allocation, is a promising operational tool for improving the safety and manageability of corridor-based UAM operations. Future work should evaluate the framework under a broader range of traffic scenarios, network configurations, and parameter settings, and should integrate rerouting with departure delays and cruise-speed control to support a more complete demand-capacity balancing framework for UAM.

Acknowledgements

This research was supported in part by the Technion Autonomous Systems Program (TASP), Technion–Israel Institute of Technology.

References

Bai, S., Sabbagh, R., Gao, Y., Li, L., and Haddad, J. (2026). Comparative evaluation of structured and unstructured urban airspace configurations for low-altitude mobility. In *Transportation research board annual meeting.* Washington, D.C..

Bauranov, A., and Rakas, J. (2021). Designing airspace for urban air mobility: A review of concepts and approaches. *Progress in Aerospace Sciences*, *125*, 100726. Retrieved from `https://www.sciencedirect.com/science/article/pii/S0376042121000312` doi: https://doi.org/10.1016/j.paerosci.2021.100726

Ben-Akiva, M., Ramming, M., and Bekhor, S. (2004, 01). Route choice models. , 23-46. doi: 10.1007/978-3-662-07809-9_2

Bijjahalli, S., Gardi, A., Pongsakornsathien, N., Sabatini, R., and Kistan, T. (2022). A unified airspace risk management framework for uas operations. *Drones*, *6*(7). Retrieved from `https://www.mdpi.com/2504-446X/6/7/184` doi: 10.3390/drones6070184

Cascetta, E., Nuzzolo, A., Russo, F., and Vitetta, A. (1996). A modified logit route choice model overcoming path overlapping problems. specification and some calibration results for interurban networks.. Retrieved from `https://api.semanticscholar.org/CorpusID:126730187`

Cohen, A. P., Shaheen, S. A., and Farrar, E. M. (2021). Urban air mobility: History, ecosystem, market potential, and challenges. *IEEE Transactions on Intelligent Transportation Systems*, *22*(9), 6074-6087. doi: 10.1109/TITS.2021.3082767

Du, S., Zhong, G., Wang, F., Pang, B., Zhang, H., and Jiao, Q. (2024). Safety risk modelling and assessment of civil unmanned aircraft system operations: A comprehensive review. *Drones*, *8*(8). Retrieved from `https://www.mdpi.com/2504-446X/8/8/354` doi: 10.3390/drones8080354

EUROCONTROL, B. (2018). Unmanned aircraft systems (uas) atm integration.

Hart, P. E., Nilsson, N. J., and Raphael, B. (1968). A formal basis for the heuristic determination of minimum cost paths. *IEEE Transactions on Systems Science and Cybernetics*, *4*(2), 100-107. doi: 10.1109/TSSC.1968.300136

He, X., He, F., Li, L., Zhang, L., and Xiao, G. (2022). A route network planning method for urban air delivery. *Transportation Research Part E: Logistics and Transportation Review*, *166*, 102872. Retrieved from https://www.sciencedirect.com/science/article/pii/S1366554522002526 doi: https://doi.org/10.1016/j.tre.2022.102872

He, X., Li, L., Mo, Y., Huang, J., and Qin, S. J. (2024). A distributed route network planning method with congestion pricing for drone delivery services in cities. *Transportation Research Part C: Emerging Technologies*, *160*, 104536. Retrieved from https://www.sciencedirect.com/science/article/pii/S0968090X24000573 doi: https://doi.org/10.1016/j.trc.2024.104536

Lee, H., Moolchandani, K. A., and Arneson, H. (2022). Demand capacity balancing at vertiports for initial strategic conflict management of urban air mobility operations. In *2022 ieee/aiaa 41st digital avionics systems conference (dasc)* (p. 1-10). doi: 10.1109/DASC55683.2022.9925753

Long, Q., Ma, J., Jiang, F., and Webster, C. (2023, 09). Demand analysis in urban air mobility: A literature review. *Journal of Air Transport Management*, *112*, 102436. doi: 10.1016/j.jairtraman.2023.102436

Meng, L., Wu, M., Wen, X., Zhou, Z., and Tian, Q. (2025). Optimization of flight scheduling in urban air mobility considering spatiotemporal uncertainties. *Aerospace*, *12*(5). Retrieved from https://www.mdpi.com/2226-4310/12/5/413 doi: 10.3390/aerospace12050413

Moolchandani, K. A., and Lee, H. (2024). Demand-capacity balancing algorithms for urban air mobility operations. In *2024 aiaa datc/ieee 43rd digital avionics systems conference (dasc)* (p. 1-9). doi: 10.1109/DASC62030.2024.10749675

NASA, C. (2021). Utm concept of operations v2. 0.

Prashker, J. N., and Bekhor, S. (2004). Route choice models used in the stochastic user equilibrium problem: A review. *Transport Reviews*, *24*(4), 437–463. Retrieved from https://doi.org/10.1080/0144164042000181707 doi: 10.1080/0144164042000181707

Quan, Q., Fu, R., and Cai, K. (2021). Practical control for multicopters to avoid non-cooperative moving obstacles. *CoRR*, *abs/2101.02889*. Retrieved from https://arxiv.org/abs/2101.02889

Safadi, Y., and Haddad, J. (2024). Overview and perspectives of air mobility operations and simulation tools. *IFAC-PapersOnLine*, *58*(10), 296-301. Retrieved from https://www.sciencedirect.com/science/article/pii/S2405896324004403 (17th IFAC Symposium on Control of Transportation Systems CTS 2024) doi: https://doi.org/10.1016/j.ifacol.2024.07.356

Song, K., and Yeo, H. (2021). Development of optimal scheduling strategy and approach control model of multicopter vtol aircraft for urban air mobility (uam) operation. *Transportation Research Part C: Emerging Technologies*, *128*, 103181. Retrieved from https://www.sciencedirect.com/science/article/pii/S0968090X21001972 doi: https://doi.org/10.1016/j.trc.2021.103181

Tang, Y., Xu, Y., and Inalhan, G. (2022). An integrated approach for on-demand dynamic capacity management service in u-space. *IEEE Transactions on Aerospace and Electronic Systems*, *58*(5), 4180-4195. doi: 10.1109/TAES.2022.3159317

Thibbotuwawa, A., Nielsen, P., Banaszak, Z., and Bocewicz, G. (2019, 01). Energy consumption in unmanned aerial vehicles: A review of energy consumption models and their relation to the uav routing: Part ii. In (p. 173-184). doi: 10.1007/978-3-319-99996-8_16

Xie, H., Wu, Y., Yin, J., Zhu, Y., Zhu, Z., and Wu, Q. (2025). Integrating raster modeling with collision risk analysis to evaluate the capacity of urban low-altitude airspace systems. *Aerospace*, *12*(12). Retrieved from https://www.mdpi.com/2226-4310/12/12/1044 doi: 10.3390/aerospace12121044

Xie, Y., Gardi, A., Liang, M., and Sabatini, R. (2023a). Ai-based dynamic re-routing for dense low-altitude air traffic management. In *2023 ieee/aiaa 42nd digital avionics systems conference (dasc)* (p. 1-10). doi: 10.1109/DASC58513.2023.10311237

Xie, Y., Gardi, A., Liang, M., and Sabatini, R. (2023b). Ai-based dynamic re-routing for dense low-altitude air traffic management. In *2023 ieee/aiaa 42nd digital avionics systems conference (dasc)* (p. 1-10). doi: 10.1109/DASC58513.2023.10311237

Xie, Y., Gardi, A., and Sabatini, R. (2021, 08). Hybrid ai-based demand-capacity balancing for uas traffic management and urban air mobility.. doi: 10.2514/6.2021-2325

Xu, Y., Prats, X., and Delahaye, D. (2020, 05). Synchronised demand-capacity balancing in collaborative air traffic flow management. *Transportation Research Part C: Emerging Technologies*, *114*, 359-376. doi: 10.1016/j.trc.2020.02.007

Yang, J., Wang, Y., Hang, X., and Delahaye, D. (2024, 01). A review on airspace design and risk assessment for urban air mobility. *IEEE Access*, *PP*, 1-1. doi: 10.1109/ACCESS.2024.3481148